Single-Turnover Kinetic Experiments Confirm the Existence of High- and Low-Affinity ATPase Sites in *Escherichia coli* Lon Protease†

Diana Vineyard, Jessica Patterson-Ward, and Irene Lee*

Department of Chemistry, Case Western Reserve University, Cleveland, Ohio 44106

Received November 21, 2005; Revised Manuscript Received January 31, 2006

ABSTRACT: Lon is an ATP-dependent serine protease that degrades damaged and certain regulatory proteins in vivo. Lon exists as a homo-oligomer and represents one of the simplest ATP-dependent proteases because both the protease and ATPase domains are located within each monomeric subunit. Previous pre-steady-state kinetic studies revealed functional nonequivalency in the ATPase activity of the enzyme [Vineyard, D., et al. (2005) *Biochemistry 44*, 1671−1682]. Both a high- and low-affinity ATPase site has been previously reported for Lon [Menon, A. S., and Goldberg, A. L. (1987) *J. Biol. Chem. 262*, 14921−14928]. Because of the differing affinities for ATP, we were able to monitor the activities of the sites separately and determine that they were noninteracting. The high-affinity sites hydrolyze ATP very slowly ($k_{obs} = 0.019 \pm 0.002$ s^{-1}), while the low-affinity sites hydrolyze ATP quickly at a rate of 17.2 ± 0.09 s^{-1}, which is comparable to the previously observed burst rate. Although the high-affinity sites hydrolyze ATP slowly, they support multiple rounds of peptide hydrolysis, indicating that ATP and peptide hydrolysis are not stoichiometrically linked. However, ATP binding and hydrolysis at both the high- and low-affinity sites are necessary for optimal peptide cleavage and the stabilization of the conformational change associated with nucleotide binding.

Lon is an ATP-dependent serine protease functioning to degrade damaged and certain regulatory proteins in vivo (*1*−*10*). Lon belongs to the ATPases associated with a variety of cellular activities (AAA^+) superfamily, whose members include ClpAP, ClpXP, ClpCP, and HslUV (*11*, *12*). They share a conserved Walker A (or P loop) and Walker B motif, which is associated with nucleotide binding and hydrolysis (*13*). Lon represents one of the simplest of the ATP-dependent proteases because both the protease and ATPase domains are located within each monomeric subunit (*14*, *15*). Crystal structures of portions of the enzyme have been recently reported and include an inactive mutant of the Lon protease domain (*16*−*18*). This structure shows Lon as a hexamer organized in a ring with a central cavity, which is commonly found in other ATP-dependent proteases (*11*, *13*, *17*). Although it is known that ATP modulates the protease activity of Lon (*4*, *5*, *7*, *19*), mechanistic details concerning how the binding and hydrolysis of ATP are coordinated with peptide bond cleavage is not known. However, it has been shown that ATP binding and hydrolysis do not affect the oligomeric state of the enzyme (*20*, *21*).

We have previously developed a continuous fluorescent peptidase assay to monitor the kinetics of peptide cleavage. Because the inner-filter effect of fluorescence interferes at high concentrations of 100% fluorescent peptide, we use S3,[1] a 10% mixture of fluorescently labeled peptide with its nonfluorescent analogue (S2) (*22*). No optical signal from the peptide is needed when monitoring ATPase activity; therefore, only the nonfluorescent analogue (S2) is used to account for the effect of the peptide (*23*). This 10 amino acid long (S3 and S2) peptide sequence contains only one cleavage site and comes from the λN protein, which is a physiological substrate of *Escherichia coli* Lon (*24*). Because our model peptide (S3 and S2) contains only one Lon cleavage site and it stimulates ATP hydrolysis, its kinetics of degradation can be directly attributed to the ATP-dependent peptidase reaction rather than polypeptide unfolding or processive peptide cleavage (*22*, *24*).

We have utilized this peptide substrate in steady-state kinetic and product inhibition studies to establish a minimal kinetic mechanism for *E. coli* Lon protease (*22*). This mechanism proposed a sequential mechanism for ATP binding and hydrolysis, which mediated peptide cleavage presumably through a predicted ATP-dependent translocation step. The resulting Lon/ATP-bound enzyme form (F) was distinct from the precatalytic Lon (E). Because the steady-state methods and predicted kinetic model could not address the microscopic details along the reaction pathway, we utilized pre-steady-state kinetic techniques to determine the timing of events as well as individual rate constants. Previously, we were able to elucidate the timing of ATP

† This work was support by the NIH Grant GM067172.

* To whom correspondence should be addressed. Telephone: 216-368-6001. Fax: 216-368-3006. E-mail: irene.lee@case.edu.

[1] Abbreviations: AMPPNP, adenylyl 5-imidodiphosphate; DTT, dithiothreitol; Abz, anthranilamide; Bz, benzoic acid amide; HBTU, *O*-benzotriazole-*N*,*N*,*N*′,*N*′-tetramethyl-uronium-hexafluoro-phosphate; HEPES, *N*-2-hydroxyethylpiperazine-*N*′-ethanesulfonic acid; KP_i, potassium phosphate; $Mg(OAc)_2$, magnesium acetate; KOAc, potassium acetate; PEI−cellulose, polyethyleneimine−cellulose; S2, a nonfluorescent analogue of S3 that is degraded by Lon identically as S3 and is used in the ATPase reactions to conserve the fluorescent peptide (S3): YRGITCSGRQK(benzoic acid amide) (Bz); S3, a mixed peptide substrate containing 10% of the fluorescent peptide $Y(NO_2)$RGITCSGRQ-K(Abz) and 90% S2.

10.1021/bi052377t CCC: $33.50
Published on Web 03/21/2006

Scheme 1: Enzyme Forms Associated with Various Concentrations of ATP[a]

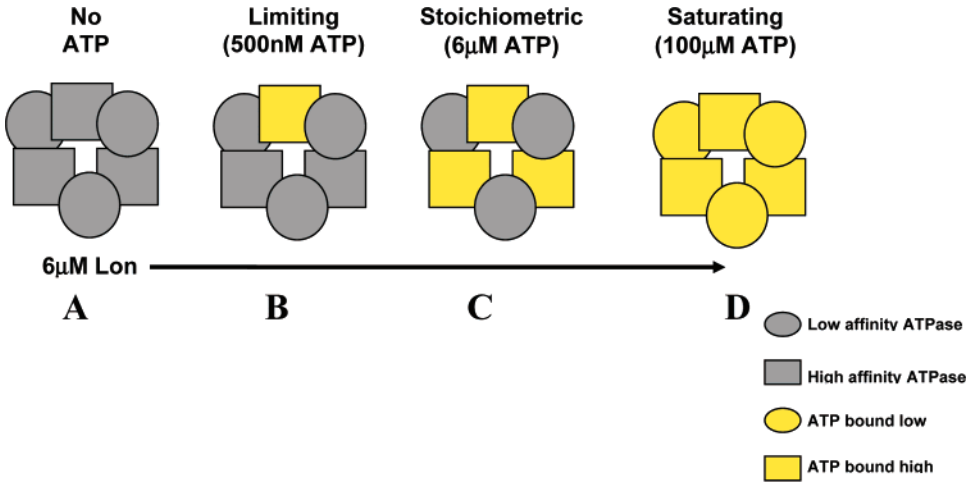

[a] Form A is a free enzyme containing two different sets of ATPase sites that are represented by gray squares and circles. Form B is formed under single-turnover conditions when only 500 nM ATP is present. The occupancy of ATP to an enzyme subunit is illustrated by the change in color from gray to yellow. Form C represents the enzyme form where only the tight sites are occupied by ATP. Form D represents an enzyme form where both the tight and weak sites are saturated with ATP.

hydrolysis and peptide cleavage in Lon (*25*), by demonstrating that ATP hydrolysis was occurring before peptide cleavage during the first turnover of Lon. This study found that *E. coli* Lon exhibits lag kinetics in the degradation of S3 but burst kinetics in ATP hydrolysis. Furthermore, the ATPase activity of Lon reveals functional nonequivalency in the subunits of the enzyme, because only 50% of the ATP bound to Lon is hydrolyzed before peptide cleavage (*25*). The observed asymmetry in the ATPase activity could be attributed to the two different classes of ATP-binding sites found in *E. coli* Lon as reported by Menon and Goldberg ($K_d < 1$ μM and $K_d \sim 10$ μM) (*26*).

Thus far, kinetic data on the ATPase-dependent degradation of the model peptide S3 by Lon implicates a reaction model by which the nonequivalent ATPase sites function cooperatively to modulate the efficiency of peptide cleavage (*25*). This model predicts that ATP hydrolysis will occur with a burst rate constant of $\sim$12 s^{-1} at the tight sites of Lon only when the low-affinity sites are occupied by ATP. Furthermore, optimal peptide hydrolysis is attained through the coordinated ATP binding to the low-affinity sites and hydrolysis at the high-affinity sites. However, this model is constructed on the basis of kinetic data obtained under pseuo-first-order conditions, where the concentration of ATP is in excess over Lon. As such, the functional roles of the high- and low-affinity ATPase sites could not be independently examined, and the validity of the proposed model could not be rigorously tested. To further investigate the cooperative function of the two kinds of ATPase sites in Lon and their respective impact on the kinetics of peptide cleavage, we monitored the ATPase and peptidase activities under limiting nucleotide concentrations, where only the high-affinity ATP-binding sites of Lon are occupied (Scheme 1). Under these conditions, although multiple rounds of peptide hydrolysis occur, the rate constant is 10-fold lower than that obtained when both ATP-binding sites are occupied under saturating levels of ATP. Dependent upon the level of ATP saturation, Lon exhibits two distinct kinetic behaviors in its ATPase sites, with optimal peptide hydrolysis occurring upon full occupancy of ATP at both of the sites. Unexpectedly, ATP hydrolysis at the high-affinity sites is stimulated by peptide or protein substrates and is independent of nucleotide binding at the low-affinity ATPase sites. Collectively, the data obtained in this study reveal that peptide cleavage is not stoichiometrically linked to ATP hydrolysis because multiple rounds of peptide hydrolysis occur under conditions of limiting ATP, where only the high-affinity sites are occupied. We have also shown that the two ATPase sites hydrolyze ATP at drastically different rates, which are seemingly unaffected by ATP hydrolysis at the other site. The previously proposed reaction model (*25*) is therefore revised accordingly to account for our currently observed data.

MATERIALS AND METHODS

Materials. ATP and casein was purchased from Sigma, whereas [α-^{32}P]ATP was purchased from Perkin−Elmer or ICN Biomedical. Fmoc-protected amino acids, Boc-anthranilamide (Abz), Fmoc-protected Lys Wang resin, and *O*-benzotriazole-*N*,*N*,*N*′,*N*′-tetramethyl-uronium-hexafluorophosphate (HBTU) were purchased from Advanced ChemTech and NovaBiochem. Tris, *N*-2-hydroxyethylpiperazine-*N*′-ethanesulfonic acid (HEPES), and polyethyleneimine−cellulose (PEI−cellulose) thin-layer chromatography (TLC) plates were purchased from Fisher.

General Methods. Peptide synthesis and protein purification procedures were performed as described previously (*24*). All enzyme concentrations were reported as Lon monomer concentrations. All reagents are reported as final concentrations.

Double-Filter-Binding Assay. For the high-affinity ATP site binding experiment, 50 nM [α-^{32}P]ATP was mixed with 0.005−6 μM Lon (*27*) in 15 μL of 50 mM HEPES at pH 8.0, 5 mM magnesium acetate [$Mg(OAc)_2$], 75 mM potassium acetate (KOAc), and 2 mM dithiothreitol (DTT). A total of 3 μL of the reactions (performed in triplicate) was spotted onto a piece of nitrocellulose mounted onto a dot-blot apparatus (BioRad) with a piece of Immobilon Ny$^+$ below as described elsewhere (*28*, *29*). All reactions were performed at least in triplicate. Each spot was washed with 10 μL of cold reaction buffer 2 times. The radioactive counts at each spot were quantified by PhosphorImaging using the Packard

Cyclone storage phosphor system. The concentration of bound was determined according to eq 1

$$[\text{bound}] = \left(\frac{NC_{dlu}}{NC_{dlu} + NY^{+}_{dlu}}\right)[[\alpha\text{-}^{32}P]ATP] \quad (1)$$

where NC_{dlu} is the radioactive count on the nitrocellulose membrane and NY^{+}_{dlu} is the radioactive count on the Immobilon Ny^{+} membrane. The binding parameters were determined by fitting the data with eq 2 using the nonlinear regression analysis program Prism (GraphPad) software version 4

$$[RL] = \frac{([R] + [L] + K_d) - \sqrt{([R] + [L] + K_d)^2 - 4[R][L]}}{2[L]} \quad (2)$$

where [L] is the concentration of [α-^{32}P]ATP, [R] is the concentration of Lon, [RL] is the concentration of [α-^{32}P]-ATP bound to Lon, and K_d is the equilibrium dissociation constant for ATP bound at the high-affinity site.

Single-Turnover ATPase Assays. Single-turnover data for ATP hydrolysis were measured as described elsewhere (*23*), and all reactions were performed at least in triplicate. Briefly, for the ATPase measurements, each reaction mixture (70 μL) contained 50 mM HEPES (pH 8.0), 75 mM KOAc, 5 mM $Mg(OAc)_2$, 5 mM DTT, and 5 or 6 μM Lon monomer. For the peptide-stimulated ATPase reactions, 500 μM peptide substrate (S2) was added to each reaction mixture and the reactions were initiated by the addition of [α-^{32}P]ATP. Subsequently, 5 μL aliquots were quenched in 10 μL of 0.5 N formic acid at 12 time points (from 0 to 15 min). A 3 μL aliquot of the reaction was spotted directly onto a PEI−cellulose TLC plate (10 × 20 cm), and the plate developed in 0.75 M potassium phosphate (KP_i) buffer (pH 3.4). Radiolabeled ADP was then quantified using the Packard Cyclone storage phosphor screen Phosphor imager purchased from Perkin−Elmer Life Science. To compensate for slight variations in spotting volume, the concentration of the ADP product obtained at each time point was corrected using an internal reference as shown in eq 3

$$[\text{ADP}] = \left(\frac{ADP_{dlu}}{ATP_{dlu} + ADP_{dlu}}\right) \times [\text{ATP}] \quad (3)$$

All assays were performed at least in triplicate, and the kinetic parameters were determined by fitting the time-course data with a single-exponential eq 4 using the nonlinear regression program Prism (Graphpad) software version 4

$$Y = A \exp^{-k_{obs}t} + C \quad (4)$$

where t is time in seconds, Y is [ADP] in micromolar, A is the amplitude in micromolar, k_{obs} is the observed rate constant in s^{-1}, and C is the end point.

Peptidase Methods. Peptidase activity was monitored on a Fluoromax 3 spectrofluorimeter (Horiba Group) as described previously (*22*). Assays contained 50 mM HEPES at pH 8.0, 75 mM KOAc, 5 mM DTT, 5 mM $Mg(OAc)_2$, 1 mM S3 peptide (excitation at 320 nm and emission at 420 nm), 5 or 6 μM Lon, and either ATP or adenylyl 5-imidodiphosphate (AMPPNP) (0−100 μM).

Chemical-Quench ATPase Activity Assays. The acid-quenched time courses for ATP hydrolysis were measured using a rapid-chemical-quench-flow instrument from KinTek Corporation as described by Vineyard et al. (*25*). All solutions were made in 50 mM HEPES buffer at pH 8.0, 5 mM DTT, 5 mM $Mg(OAc)_2$, and 75 mM KOAc. A 15 μL buffered solution of 6 μM Lon monomer or 6 μM Lon preincubated with 6 μM ATP, with and without 500 μM S2 or 20 μM casein, was rapidly mixed with a 15 μL buffered solution of 100 μM ATP containing 0.01% of [α-^{32}P]ATP at 37 °C for varying times (0−3 s). The reactions were quenched with 0.5 N formic acid and then extracted with 200 μL of phenol/chloroform/isoamyl alcohol at pH 6.7 (25:24:1). A 3 μL aliquot of the aqueous solution was spotted directly onto a PEI−cellulose TLC plate and treated as above. All assays were performed at least in triplicate, and the average of those traces was used for data analysis. The burst amplitudes and burst rates were determined by fitting the k_{obs} data from 0 to 400 ms with eq 5

$$Y = A \exp^{-k_{burst}t} + C \quad (5)$$

where t is time in seconds, Y is [ADP] in micromolar, A is the burst amplitude in micromolar, k_{burst} is the burst rate constant in s^{-1}, and C is the end point. The observed steady-state rate constants ($k_{ss,ATP}$) were determined by fitting the data from 600 ms to 3 s with the linear function, $Y = mX + C$, where X is time, Y is [ADP]/[Lon], m is the observed steady-state rate constant in s^{-1}, and C is the y intercept. Data fitting was accomplished using the nonlinear regression program Prism (GraphPad) software version 4.

Tryptic Digestions. Tryptic digest reactions in mixtures containing 6 μM Lon, 50 mM HEPES (pH 8.0), 5 mM magnesium acetate, 2 mM DTT, ±500 μM S2 peptide, and either 1 mM ATP, 6 μM ATP, or 500 nM ATP were started by the addition of 1/50 (w/w) TPCK (*N*-*p*-tosyl-L-phenylalanine chloromethyl ketone)-treated trypsin with respect to Lon. At 0, 2, 4, 20, and 40 min, a 3 μL reaction aliquot was quenched in 3 μg of soybean trypsin inhibitor (SBTI) followed by boiling. The quenched reactions were then resoved by 12.5% SDS−PAGE analysis and visualized with Coomassie brilliant blue.

RESULTS

Examining Binding of the ATPase Sites in Lon. Although *E. coli* Lon contains one ATP-binding domain in each of its monomeric subunits, the existence of both a high- and low-affinity ATP-binding site is evident in its oligomeric form (*25*, *26*). To verify the existence of two different ATPase sites in Lon under our reaction conditions, we measured the affinities of Lon for [α-^{32}P]ATP using a filter-binding assay adapted from the protocols of Jia et al. and Gilbert and Mackey (*27*, *28*) and Wong and Lohman (*29*). The half-life of the complex, where ATP is bound at the low-affinity sites, can be calculated using the off rate of ATP (Vineyard, D., and Lee, I., manuscript in preparation). Because the half-life is on a millisecond time scale, the filter-binding assay is not an appropriate method for detecting the affinity of ATP to the low-affinity site. However, the binding to this site has previously been determined under our reaction conditions using steady-state kinetic methods (*22*), and the resulting affinity agreed with the published value of 10 μM

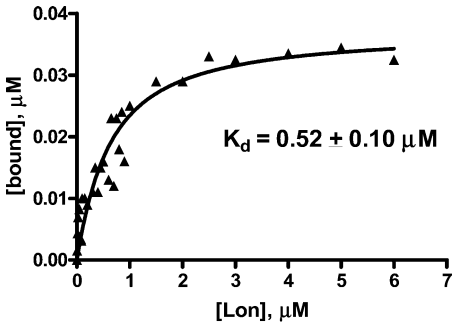

FIGURE 1: Determining the K_d for the high-affinity ATPase site in E. coli Lon using an adapted filter-binding assay. To monitor the binding of [α-^{32}P]ATP to only the high-affinity site, various concentrations of Lon (0.005−6 μM) were incubated with 50 nM [α-^{32}P]ATP at 4 °C. The amount of the Lon/[α-^{32}P]ATP complex formed was quantified by PhosphorImaging of the nitrocellulose membrane, and the free [α-^{32}P]ATP was quantified by PhosphorImaging of the positively charged Immobilon Ny$^+$ membrane. The amount of (bound) complex (▲) was calculated as described in the Materials and Methods, and the generated data were fit using a binding isotherm (eq 2). The resulting K_d value was 0.52 ± 0.096 μM for the high-affinity site.

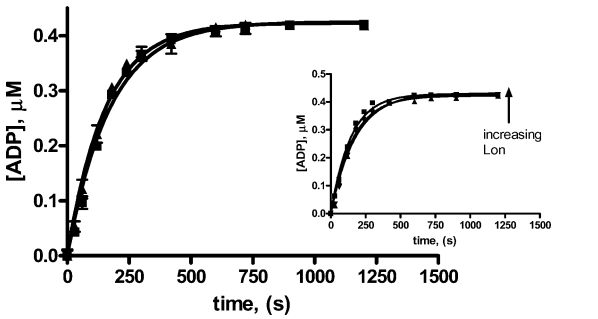

FIGURE 2: Pre-steady-state time courses of ATPase activity of *E. coli* Lon under single-turnover conditions. The time courses for ATP hydrolysis at the high-affinity sites were determined by incubating 5 μM Lon with 500 nM [α-^{32}P]ATP in the absence (■) and presence (▲) of 500 μM S2 peptide. The reactions were quenched with acid at the indicated times, and the concentrations of [α-^{32}P]ADP were determined by TLC followed by PhosphorImaging. The k_{obs} values were determined by fitting the time courses using a single-exponential equation as described in the Materials and Methods, yielding observed rate constants of 0.006 ± 0.004 and 0.007 ± 0.003 s^{-1} in the absence and presence of the S2 peptide, respectively. The inset shows time courses for 500 nM [α-^{32}P]ATP hydrolysis at the high-affinity sites in the presence of 500 μM S2 peptide at increasing concentrations of Lon: 5 μM (▲), 7 μM (◆), and 10 μM (□). The k_{obs} values were determined by fitting the time courses using a single-exponential equation as described in the Materials and Methods, yielding observed rate constants of 0.007 ± 0.001, 0.007 ± 0.001, and 0.006 ± 0.001 s^{-1}, respectively.

by Menon and Goldberg (*26*). The equilibrium dissociation constant for the high-affinity site was never specifically determined because of the limit of detection of the previous assays (K_d < 1μM) (*26*). Therefore, we utilized the filter-binding assay to better define the binding affinity of Lon to the high-affinity ATPase site.

To probe the high-affinity site, 50 nM [α-^{32}P]ATP was incubated with varying amounts of Lon and the resulting Lon/[α-^{32}P]ATP complex was immobilized onto a nitrocellulose membrane, whereas unbound [α-^{32}P]ATP was trapped by a positively charged nylon membrane placed directly below the nitrocellulose filter. The concentration of Lon was varied rather than [α-^{32}P]ATP to eliminate the high background generated when the concentration of [α-^{32}P]ATP is increased because the concentration Lon is held constant in the nanomolar range. A binding isotherm of the high-affinity ATP site in Lon was generated by quantifying the amount of ^{32}P immobilized onto the nitrocellulose versus the nylon membrane as described in the Materials and Methods. As shown in Figure 1, the binding of ATP at the high-affinity site was detected with a K_d value of 0.52 ± 0.096 μM. Control experiments were performed to ensure that no [α-^{32}P]ATP hydrolysis was occurring under the reaction conditions (data not shown). These results are consistent with the earlier observation reported by Menon and Goldberg (*26*) that Lon contains two affinities for ATP, which differ from one another by approximately 10-fold.

Examining Activity of the High-Affinity ATPase Sites of Lon. Kinetic analyses performed under pseudo-first-order conditions, where ATP is in excess over the enzyme concentration, have revealed an apparent functional asymmetry in the ATPase sites (*25*). We examined the ATPase activity of the high- and low-affinity sites independently of one another by manipulating the concentration of nucleotide such that either just the high-affinity sites or both sets of sites were occupied. To monitor the ATPase activity at the high-affinity sites of Lon, single-turnover experiments were employed. When the concentrations of the reactants are adjusted such that the Lon concentration (5 μM) is in excess over limiting ATP (500 nM), only the high-affinity sites are occupied by the nucleotide (K_d = 0.52 μM, see above). Enzyme forms A−D (Scheme 1) represent different ATP-bound states of Lon under the various reaction conditions used in this study. The proposed enzyme form under limiting ATP conditions is shown as the enzyme form B in Scheme 1 (*17*); thus, we can selectively monitor ATP hydrolysis at only the high-affinity sites. The inset of Figure 2 shows the hydrolysis of ATP at the high-affinity sites as Lon is increased (5, 7, and 10 μM). The observed rate constants range from 0.006 to 0.007 s^{-1} with a standard deviation of less than 0.8%. Because the rate constants are identical, the binding of ATP is not rate-limiting under the single-turnover reaction conditions employed in the experiment. Furthermore, as shown in Figure 2, the presence of the S2 peptide does not influence ATP hydrolysis at the high-affinity sites because the rate constant for the reaction is 0.006 ± 0.0004 and 0.007 ± 0.0003 s^{-1} in the absence and presence of a saturating amount of S2 (500 μM), respectively. This is consistent with our previous observation that the burst rate constant associated with ATP hydrolysis under pseudo-first-order conditions was not affected by the presence of the S2 peptide (*25*). The rate constant for S2-stimulated ATP hydrolysis at the high-affinity sites under single-turnover conditions (k_{obs} = 0.007 ± 0.0003 s^{-1}), however, is considerably slower than the burst rate obtained when ATP was in excess over the enzyme concentration (k_{burst} = 11.3 ± 3.3 s^{-1}) (*25*). These two experiments differ only by the occupancy of ATP at the low-affinity sites. This implies that, although one ATP-binding site exists per monomer, two functionally distinct ATPase sites are evident in the homo-oligomeric form of Lon.

Because the hydrolysis at the high-affinity ATPase sites is minimal and ATP hydrolysis is required for optimal peptide cleavage (*23*), we questioned whether the catalytic efficiency of S3 cleavage is coupled with ATP hydrolysis

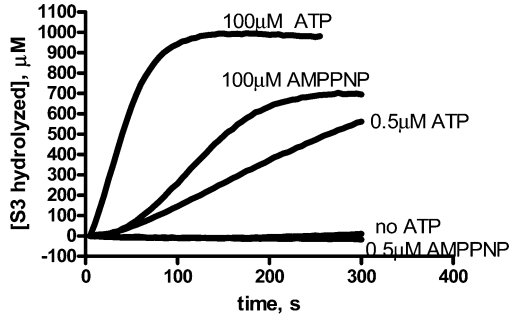

FIGURE 3: S3 hydrolysis by *E. coli* Lon under limiting nucleotide conditions. The 5 μM Lon monomer was incubated with 1 mM S3 peptide in the presence of 0, 0.5, and 100 μM ATP and 0.5 and 100 μM AMPPNP. The fluorescence changes associated with peptide cleavage were converted to product concentrations as described in the Materials and Methods. The k_{obs} values associated with each trace are summarized in Table 1.

Table 1: Rate Constants Associated with Peptidase Activity

	[nucleotide] (μM)	$k_{obs,S3}$ (s^{-1})
limiting ATP	0.5	0.32 ± 0.07
stoichiometric ATP	5	1.52 ± 0.05
saturating ATP	100	2.69 ± 0.30
saturating AMPPNP	100	0.96 ± 0.08

at the high-affinity sites. To address this issue, we monitored the kinetics of S3 cleavage under single-turnover conditions, where ATP is limiting (5 μM Lon, 500 nM ATP, and 1 mM S3). Under these conditions, the predominant enzyme form is homo-oligomeric Lon, with ATP bound only at the high-affinity sites (enzyme form B in Scheme 1). As shown in Figure 3, although the rate constant for S3 cleavage at limiting ATP concentrations (Table 1, $k_{obs,S3} = 0.32\ s^{-1}$) is slower than with saturating ATP, enzyme form D in Scheme 1 (Table 1, $k_{obs,S3} = 2.69\ s^{-1}$), Lon is undergoing multiple rounds of peptide cleavage with only limiting amounts of ATP. Because no peptide hydrolysis occurs in the presence of limiting amounts of the nonhydrolyzable ATP analogue, AMPPNP, (Figure 3) at least one molecule of ATP must be hydrolyzed for peptide cleavage to occur under these conditions. Although, nonstoichiometric processing of ATP and the S3 peptide is observed under saturating (100 μM) ATP conditions, the single-turnover data much more clearly demonstrate that ATP and peptide hydrolysis are not stoichiometric. As previously reported and shown here in Figure 3 for a comparison to the limiting nucleotide conditions, saturating amounts of AMPPNP (100 μM) support S3 hydrolysis at a lower rate than under saturating ATP conditions (100 μM; Table 1) (*22*). In this case, saturating AMPPNP most likely supports slow peptide hydrolysis because its binding at the low-affinity sites in addition to not generating ADP from the lack of hydrolysis is sufficient to lock Lon into an active conformation (*22*).

Binding and Hydrolysis of ATP at the Tight Sites Are Independent of Nucleotide Binding and Hydrolysis at the Weak Sites. To further probe the functional nonequivalency of the two ATPase sites, the activity of each site was monitored independently of the other using radiolabeled ATP as a selective probe. Because the K_d for binding ATP at the high-affinity sites was 0.52 ± 0.096 μM, the single-turnover experimental conditions employed above were not sufficient to saturate those sites. To detect the full effect of ATP hydrolysis when the high-affinity sites were fully occupied,

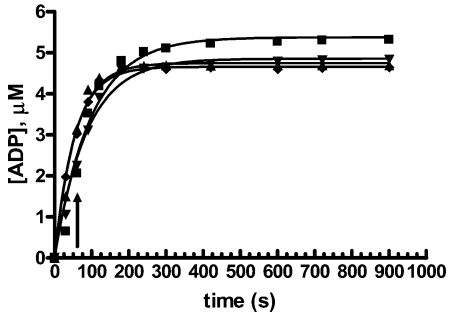

FIGURE 4: Representative *E. coli* Lon time courses of ATP hydrolysis at the high-affinity sites. [α-^{32}P]ATP (6 μM) was incubated with 6 μM monomeric Lon in the absence (■) or presence (▲) of 500 μM S2 peptide and quenched with acid at varying time points. To see the effect of nucleotide occupation at the low-affinity sites on the high-affinity site ATP hydrolysis, 100 μM ATP was added at 1 half-life into the reaction 60 s in both the absence (▼) and presence (◆) of 500 μM S2 peptide to saturate the low-affinity ATPase sites. The time of addition of the 100 μM ATP in traces ▼ and ◆ is indicated by the arrow. As described in the Materials and Methods, the time courses were fit using the equation $Y = A\exp^{(-k_{obs,ATP}t)} + C$, where A is the amplitude, $k_{obs,ATP}$ is the observed rate constant, and C is the endpoint. The resulting rate constants are summarized in Table 2. The time points reported are an average of at least three different trials.

Table 2: Rate Constants Associated with High-Affinity Site ATPase Activity

	intrinsic $k_{obs,ATP}$ (s^{-1})	S2 stimulated $k_{obs,ATP}$ (s^{-1})
stoichiometric ATP	0.011 ± 0.001	0.019 ± 0.002
100 μM ATP chase	0.012 ± 0.001	0.017 ± 0.001
100 μM AMPPNP chase	0.010 ± 0.001	0.014 ± 0.001
100 μM ADP chase	0.015 ± 0.001	0.017 ± 0.001

the concentration of [α-^{32}P]ATP was raised to approximately 10-fold excess of the K_d (6 μM), which is stoichiometric to the amount of Lon in the reaction. Shown as enzyme form C in Scheme 1, under these conditions, it is assumed that the high-affinity sites are saturated and the low-affinity sites are left unoccupied.

The experiment shown in Figure 4 shows the effect on ATP hydrolysis at the high-affinity sites when the low-affinity sites were subsequently occupied with unlabeled nucleotide. To accomplish this, ATP hydrolysis was measured at the high-affinity sites under stoichiometric [α-^{32}P]-ATP/Lon conditions (enzyme form C in Scheme 1), while saturating (100 μM) unlabeled ATP was subsequently added or chased to occupy the weak-affinity sites 1 min into the reaction (enzyme form D in Scheme 1). When the experiment is performed in this manner, the hydrolysis at the high-affinity sites can be monitored for the first half-life of the reaction and then the effect of nucleotide occupation at the low-affinity sites on this hydrolysis can subsequently be seen. To ensure that 60 s was an appropriate time to add saturating nucleotide, a control experiment was done where the saturating nucleotide was added at 10 s and no difference was noted (data not shown). The rate constants associated with the hydrolysis of [α-^{32}P]ATP at the high-affinity sites alone as well as after subsequent occupation of the low-affinity sites with nucleotide are summarized in Table 2. These experiments were performed in both the presence (S2 stimulated) and absence (intrinsic) of the S2 peptide substrate to account for effects of any interaction between the ATPase

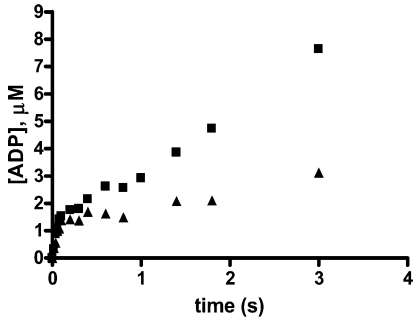

FIGURE 5: *E. coli* Lon pre-steady-state chemical-quenched time courses of ATP hydrolysis at the low-affinity sites. [α-^{32}P]ATP (100 μM) was incubated with 6 μM monomeric Lon (■) or 6 μM monomeric Lon preincubated with 6 μM ATP (▲) in the presence of 500 μM S2 peptide as described in the Materials and Methods. The preincubation of 6 μM Lon with 6 μM ATP presumably resulted in 6 μM Lon/6 μM ADP, where the high-affinity ATPase sites were saturated. The reactions were quenched with acid at the indicated times, and the concentrations of [α-^{32}P]ADP generated in the reactions were determined by TLC followed by PhosphorImaging. The time courses from 0 to 400 ms were fit with the equation $Y = A\ \exp^{(-k_{burst}t)} + C$, where A is the burst amplitude, k_{burst} is the observed burst rate constant, and C is the endpoint. The resulting k_{burst} for Lon (■) was 15.9 ± 0.07 s^{-1}, and the resulting k_{burst} for 1 Lon/1 ADP (▲) was 17.2 ± 0.09 s^{-1}. The $k_{ss,ATP}$ values were obtained by fitting the time courses from 600 ms to 3 s with a linear function and dividing the slope by the [Lon] in the reaction and were 0.40 ± 0.021 s^{-1} for Lon (■) and 0.11 ± 0.014 s^{-1} for 1 Lon/1 ADP (▲). The time points reported here are an average of at least three different trials.

and peptidase activities. As illustrated in Table 2, the observed rate constant for ATP hydrolysis at the high-affinity sites was unaffected by the occupation of the low-affinity sites 60 s into the reaction with ATP (Figure 4), AMPPNP (figure not shown), or ADP (figure not shown). Because both a nonhydrolyzable ATP analogue (AMPPNP) and a product inhibitor (ADP) were also tested, these data indicate that ATP hydrolysis at the high-affinity sites is independent of ATP binding and/or hydrolysis at the low-affinity sites. The rate constant for ATP hydrolysis at the high-affinity sites was slightly faster in the presence of the S2 peptide (Table 2) and casein (data not shown), thus suggesting that communication occurs as a result of the peptide or protein interacting with the high-affinity ATPase site of Lon.

Peptide and Protein Substrates Stimulate ATP Hydrolysis at the High-Affinity Sites. In the previous experiment, which was depicted in Figure 4 for ATP, 100 μM AMPPNP, ATP, and ADP did not compete out the [α-^{32}P]ATP bound at the high-affinity sites because the amplitudes of the time courses were unaffected. The converse experiment could then be employed to monitor ATP hydrolysis at the low-affinity sites. In this experiment, Lon (6 μM) was preincubated with a stoichiometric amount of unlabeled ATP (6 μM; enzyme form C in Scheme 1). During this preincubation, only the high-affinity sites are occupied with unlabeled ATP, which was hydrolyzed to ADP that remains bound at the high-affinity sites. As such, the subsequent hydrolysis of 100 μM [α-^{32}P]ATP by Lon would directly reflect the ATPase activity at the low-affinity sites. To ensure that the ATP hydrolysis at the high-affinity sites, which occurred during the preincubation, was not necessary, the experiment was also performed where Lon (6 μM) was preincubated with ADP (6 μM) and the traces were identical (data not shown). Figure 5 shows the hydrolysis of [α-^{32}P]ATP at the low-affinity sites when the high-affinity sites are occupied by unlabeled ADP (▲). Hydrolysis of [α-^{32}P]ATP at the low-affinity sites exhibited an initial burst in [α-^{32}P]ADP production, which when fit using eq 6 from the Materials and Methods, yielded an observed burst rate constant of 17.2 ± 0.09 s^{-1} (▲), which is comparable to the value of 15.9 ± 0.07 s^{-1} (■), where both the high- and low-affinity sites are contributing. As expected, the rate constant obtained here, 15.9 ± 0.07 s^{-1} (■), agrees well with the previously determined value of 11.3 ± 3.3 s^{-1} (*25*). The pre-steady-state time course showing the hydrolysis of ATP at only the low-affinity ATPase sites (▲) mirrored the pre-steady-state time course reflecting activity at both sites (■). This would imply that the pre-steady-state burst in ADP production is coming from only the low-affinity ATPase sites. As noted in the previous publication, the ATPase burst activity of Lon is unusual because it shows half-burst amplitude and the time course is triphasic (*25*). The triphasic time course showed a burst in ADP production followed by an intermediate slow phase, and then steady-state ATP turnover occurs. The time courses, therefore, cannot be fit using the classical burst equation because of the intermediate slow phase. As described in the Materials and Methods, the time courses are instead split into the pre-steady-state burst phase, which is fit using a single-exponential equation, and a linear steady-state phase.

The kinetics of each site has been monitored in the presence and absence of nucleotide occupation at the other site, and the occupancy of ADP at the high-affinity sites does not affect ATP hydrolysis at the low-affinity sites. Therefore, we have now demonstrated that the ATPase sites hydrolyze ATP independently of one another and the rate of ATP hydrolysis at the high-affinity sites is much slower. This behavior explains the triphasic time courses observed in the pseudo-first-order experiments as well as the independence of the burst rate constant on the concentration of ATP, which have been previously noted (*25*). Taken together with the pre-steady-state characterization of peptide cleavage determined previously, we conclude that ATP hydrolysis occurs at the low-affinity sites prior to S3 cleavage.

Interestingly, there is an observed 4-fold stimulation in the steady-state rate in the presence of S2 peptide (Figure 5) or the unstructured protein substrate casein (*30*, *31*; data not shown). This is consistent with the stimulation observed in the k_{cat} for ATPase activity (*23*), but it is only observed when the high-affinity sites are not occupied by ADP (Figure 4, $k_{ss,ATP}$ = 0.40 ± 0.021 s^{-1}, ■; $k_{ss,ATP}$ = 0.11 ± 0.014 s^{-1}, ▲). This supports the implication that, although the hydrolysis at the high-affinity sites is unaffected by nucleotide occupation at the low-affinity sites, it is affected by the presence of the peptide or protein substrate.

Optimal Peptidase Activity Requires ATP Binding and Hydrolysis at Both Sites. Communication occurring between the high-affinity ATPase sites and the S2 peptide or protein substrate has been suggested by the experiments performed above. Therefore, the catalytic efficiency of S3 cleavage was examined under stoichiometric Lon/ATP conditions as well (enzyme form C in Scheme 1). The kinetics of S3 cleavage were monitored under conditions where the high-affinity sites were saturated with ATP (5 μM Lon, 5 μM ATP, and 1 mM S3), and the proposed enzyme form is shown in Scheme 1. The rate constants for peptide hydrolysis under these conditions are summarized in Table 1. Because the rate at

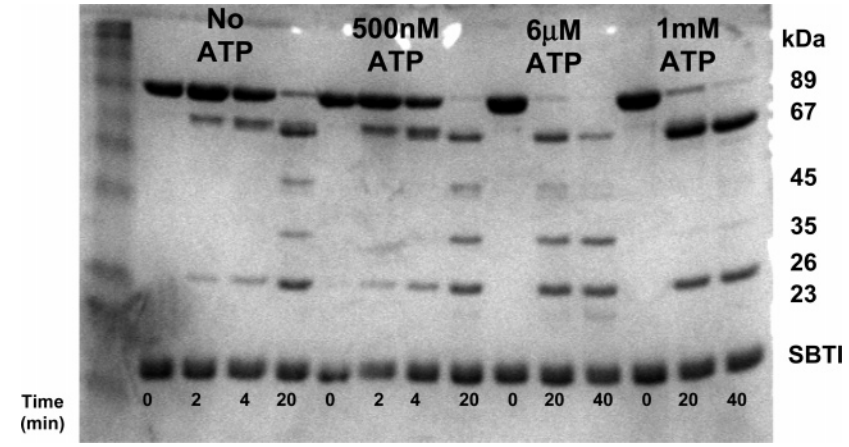

FIGURE 6: Limited tryptic digestion of Lon in the presence of varying amounts of ATP. Lon in the presence of 500 μM S2 peptide was digested with a limiting amount of trypsin and quenched at the indicated times with SBTI as described in the Materials and Methods. The first lane shows the molecular markers in kilodaltons (from top to bottom): 172, 110, 79, 62, 48, 37, 24, and 19.

100 μM ATP (enzyme form D in Scheme 1) is faster than at 5 μM ATP (enzyme form C in Scheme 1), both ATPase sites are contributing to the peptidase activity. Optimal peptide degradation is consequently recovered by the low-affinity site ATPase activity. This means that the maximal rate of peptide degradation is attained only when both the high- and low-affinity sites are saturated with ATP. Because peptidase activity is slower in the presence of the non-hydrolyzable analogue, AMPPNP, ATP binding as well as hydrolysis at the low-affinity sites are a necessity for optimal peptidase activity.

Tryptic Digest Probes the Conformational Change Associated with ATP Binding. Previously (*23*), we utilized limited tryptic digestion to probe the functional role of nucleotide binding to Lon. We detected an adenine-specific conformational change at saturating amounts of nucleotide. Although the digestion yielded a pattern of bands ranging in size from 7 to 67 kDa, the adenine-specific conformational change was monitored primarily by the detection of a stable 67 kDa fragment. When sequenced, the 67 kDa fragment included all domains of Lon (ATPase, SSD, and peptidase), except the amino-terminal region. Of all of the nucleotides tested in that study, ATP was shown to be the best activator of the peptidase activity of Lon. Therefore, it was concluded that the adenine-specific conformational change contributed to maintaining the optimal catalytic efficiency of S3 cleavage.

In light of the detection of functional nonequivalency in the ATP binding and hydrolysis activity in Lon, in this study, we questioned whether the previously observed conformational change upon nucleotide binding could be assigned to a specific interaction between ATP with either the high- or low-affinity ATPase sites in Lon. To address this issue, we subjected 6 μM Lon to limited tryptic digestion in the presence of limiting (500 nM; enzyme form B in Scheme 1), stoichiometric (6 μM; enzyme form C in Scheme 1), and excess (1 mM) amounts of ATP (enzyme form D in Scheme 1) to see the effect on the stability of the adenine-specific conformational change when one or both ATPase sites were occupied. On the basis of the two K_d values of ATP, we anticipated that only the tight sites of Lon were occupied by ATP in the first two cases. Figure 6 shows the Lon fragments generated over increasing time in the presence of the S2 peptide under conditions of no nucleotide (lanes 2−5), limiting (500 nM) ATP (lanes 6−9), stoichiometric (6 μM) ATP (lanes 10−12), and saturating (1 mM) ATP (lanes 13−15). The digest pattern was identical in the absence of the S2 peptide (data not shown). In accordance with what was previously observed, limited tryptic digestion of Lon in the presence of ATP yields fragments varying from 23 to 67 kDa. As indicated by these data, the 67 kDa fragment is substantially stabilized only by full occupation of the low-affinity ATP sites. Because binding and hydrolysis of ATP at all ATPase sites are also necessary for optimal peptidase activity in Lon, a correlation between this adenine-specific conformational change and accessibility for peptide cleavage could exist.

DISCUSSION

In this study, we utilized kinetic techniques to better understand the function of the two nonequivalent ATPase sites in *E. coli* Lon protease and their coordination with the protease activity of the enzyme. Despite being a homo-oligomer, with one ATP-binding site per monomer, Lon contains two types of ATPase sites that are functionally or kinetically distinct from one another. As such, the kinetic characterization of the activities of the ATPase sites is imperative because they are structurally indistinguishable. The experiments represented in Figure 4 demonstrate that ATP hydrolysis at the high-affinity site is unaffected by the occupation of nucleotide at the low-affinity site, while the experiments exemplified in Figure 5 show that hydrolysis of ATP at the low-affinity site is unaffected by the occupation of nucleotide at the high-affinity site. Therefore, the kinetic data support the conclusion that the two ATPase sites are functioning independent of the other. Our kinetic experiments have also allowed us to examine the coupling of the ATPase and peptidase activities of Lon protease, which are not yet fully understood. Mechanistic studies of other enzymes including Rho protein (*32*, *33*), multidrug-resistance-associated protein (MRP1) (*34*), *P*-glycoprotein (PGP) (*35*), F1-ATPase (*36*), Na^+/K^+ ATPase (*37*), topoisomerase II (*38*, *39*), and Rep helicase (*40*) have also revealed the functional roles of multiple ATPase sites.

Previously, this lab has constructed a minimal kinetic model to account for the ATP-dependent S3 cleavage by Lon using steady-state kinetics (*22*). Although this model was constructed assuming monomeric Lon subunits had equivalent ATPase activity, the order of events has been confirmed

by our current pre-steady-state kinetic studies. This minimal kinetic model predicted ATP hydrolysis to occur prior to peptide cleavage. Current as well as previous pre-steady-state kinetic studies (*25*) are consistent with this model because *E. coli* Lon exhibits lag kinetics in the degradation of the model peptide (S3) and burst kinetics in ATP hydrolysis. The burst kinetics indicate a rapid buildup of a reaction intermediate with a rate-limiting step following chemistry in the reaction pathway, while the lag kinetics for S3 peptide degradation are consistent with a need for an accumulation of a reaction intermediate prior to peptide hydrolysis. The burst kinetics for ATP hydrolysis demonstrated triphasic behavior, where only 50% of the Lon monomer was hydrolyzed in the duration of the lag in peptidase activity. Although this unusual behavior suggested the contribution of two ATPase activities, it could not separate the two.

The present study has confirmed the existence of two ATPase sites in Lon and that their activities are independent of one another. We have now demonstrated with additional pre-steady-state experiments that the ATP bound to the low-affinity sites is hydrolyzed during the lag in peptide cleavage with a burst rate constant of $17.2 \pm 0.09\ s^{-1}$. The peptide is concomitantly cleaved with a rate constant of $2.69 \pm 0.30\ s^{-1}$, while the ATP bound at the high-affinity sites is slowly being hydrolyzed with an observed rate constant of $0.019 \pm 0.002\ s^{-1}$. The previously determined minimal kinetic model also predicted a Lon/ATP-bound "F" form of the enzyme following peptide cleavage, which could undergo multiple rounds of peptide hydrolysis before reverting back to the free enzyme (*22*). This is consistent with our data in Figure 3, which demostrate that peptide and ATP hydrolysis are not stoichiometrically linked. It is still not clear how the enzyme turns over once it reaches the "F" form. Our revised mechanism for the ATPase activity in Lon predicts that the two ATPase sites are hydrolyzing ATP sequentially but are not communicating. However, binding and hydrolysis of ATP at both the high- and low-affinity ATPase sites are necessary for optimal peptide or protein degradation. The energy generated from ATP hydrolysis at the low-affinity sites could be used to translocate the protein substrate or may be used to induce a conformational change in the oligomer that facilitates protein cleavage. Therefore, the development of an effective continuous assay to measure protein degradation is currently underway to determine how the high- and low-affinity ATPase sites are contributing to protease activity.

Because the protease activity is ultimately limited by turnover of ATP hydrolysis, further kinetic characterization needs to be performed to delineate the ATPase mechanism. We and others (*4*) have previously suggested that ADP release was the rate-limiting step along the reaction pathway because it is a potent inhibitor of peptidase activity ($K_{i,ADP} = 0.3\ \mu M$) (*22*). The burst kinetics associated with ATP hydrolysis would be consistent with this, because they indicated that a step following chemistry is rate-limiting. However, the rapid-quench experiment shown in Figure 5 showed that ATP did not compete out ADP bound to the high-affinity sites of Lon, suggesting that ADP is perhaps only inhibiting at the high-affinity sites. Experiments to determine other microscopic rate constants along the ATPase reaction pathway including ADP release are currently underway to determine the rate-limiting step of the reaction.

ACKNOWLEDGMENT

We thank Dr. Anthony Berdis for his assistance and careful reading of this manuscript.

REFERENCES

1. Charette, M. F., Henderson, G. W., and Markovitz, A. (1981) ATP hydrolysis-dependent protease activity of the lon (capR) protein of *Escherichia coli* K-12, *Proc. Natl. Acad. Sci. U.S.A. 78*, 4728−4732.
2. Chung, C. H., and Goldberg, A. L. (1981) The product of the lon (capR) gene in *Escherichia coli* is the ATP-dependent protease, protease La, *Proc. Natl. Acad. Sci. U.S.A. 78*, 4931−4935.
3. Goff, S. A., and Goldberg, A. L. (1985) Production of abnormal proteins in *E. coli* stimulates transcription of lon and other heat shock genes, *Cell 41*, 587−595.
4. Goldberg, A. L., Moerschell, R. P., Chung, C. H., and Maurizi, M. R. (1994) ATP-dependent protease La (lon) from *Escherichia coli*, *Methods Enzymol. 244*, 350−375.
5. Goldberg, A. L., and Waxman, L. (1985) The role of ATP hydrolysis in the breakdown of proteins and peptides by protease La from *Escherichia coli*, *J. Biol. Chem. 260*, 12029−12034.
6. Gottesman, S. (1996) Proteases and their targets in *Escherichia coli*, *Annu. Rev. Genet. 30*, 465−506.
7. Gottesman, S., Gottesman, M., Shaw, J. E., and Pearson, M. L. (1981) Protein degradation in *E. coli*: The Ion mutation and bacteriophage λ N and cll protein stability, *Cell 24*, 225−233.
8. Gottesman, S., and Maurizi, M. R. (1992) Regulation by proteolysis: Energy-dependent proteases and their targets, *Microbiol. Rev. 56*, 592−621.
9. Maurizi, M. R. (1992) Proteases and protein degradation in *Escherichia coli*, *Experientia 48*, 178−201.
10. Schoemaker, J. M., Gayda, R. C., and Markovitz, A. (1984) Regulation of cell division in *Escherichia coli*: SOS induction and cellular location of the sulA protein, a key to lon-associated filamentation and death, *J. Bacteriol. 158*, 551−561.
11. Ogura, T., and Wilkinson, A. J. (2001) AAA+ superfamily ATPases: Common structure—Diverse function, *Genes Cells 6*, 575−597.
12. Kunau, W. H., Beyer, A., Franken, T., Gotte, K., Marzioch, M., Saidowsky, J., Skaletz-Rorowski, A., and Wiebel, F. F. (1993) Two complementary approaches to study peroxisome biogenesis in *Saccharomyces cerevisiae*: Forward and reversed genetics, *Biochimie 75*, 209−224.
13. Neuwald, A. F., Aravind, L., Spouge, J. L., and Koonin, E. V. (1999) AAA+: A class of chaperone-like ATPases associated with the assembly, operation, and disassembly of protein complexes, *Genome Res. 9*, 27−43.
14. Amerik, A., Chistiakov, L. G., Ostroumova, N. I., Gurevich, A. I., and Antonov, V. K. (1988) Cloning, expression and structure of the functionally active shortened lon gene in *Escherichia coli*, *Bioorg. Khim. 14*, 408−411.
15. Chin, D. T., Goff, S. A., Webster, T., Smith, T., and Goldberg, A. L. (1988) Sequence of the lon gene in *Escherichia coli*. A heat-shock gene which encodes the ATP-dependent protease La, *J. Biol. Chem. 263*, 11718−11728.
16. Botos, I., Melnikov, E. E., Cherry, S., Khalatova, A. G., Rasulova, F. S., Tropea, J. E., Maurizi, M. R., Rotanova, T. V., Gustchina, A., and Wlodawer, A. (2004) Crystal structure of the AAA+ α domain of *E. coli* Lon protease at 1.9 Å resolution, *J. Struct. Biol. 146*, 113−122.
17. Botos, I., Melnikov, E. E., Cherry, S., Tropea, J. E., Khalatova, A. G., Rasulova, F., Dauter, Z., Maurizi, M. R., Rotanova, T. V., Wlodawer, A., and Gustchina, A. (2004) The catalytic domain of *Escherichia coli* Lon protease has a unique fold and a Ser-Lys dyad in the active site, *J. Biol. Chem. 279*, 8140−8148.
18. Li, M., Rasulova, F., Melnikov, E. E., Rotanova, T. V., Gustchina, A., Maurizi, M. R., and Wlodawer, A. (2005) Crystal structure of the N-terminal domain of *E. coli* Lon protease, *Protein Sci. 14*, 2895−2900.
19. Menon, A. S., Waxman, L., and Goldberg, A. L. (1987) The energy utilized in protein breakdown by the ATP-dependent protease (La) from *Escherichia coli*, *J. Biol. Chem. 262*, 722−726.
20. Rudyak, S. G., Brenowitz, M., and Shrader, T. E. (2001) Mg^{2+}-linked oligomerization modulates the catalytic activity of the Lon (La) protease from *Mycobacterium smegmatis*, *Biochemistry 40*, 9317−9323.

21. van Dijl, J. M., Kutejova, E., Suda, K., Perecko, D., Schatz, G., and Suzuki, C. K. (1998) The ATPase and protease domains of yeast mitochondrial Lon: Roles in proteolysis and respiration-dependent growth, *Proc. Natl. Acad. Sci. U.S.A. 95*, 10584−10589.
22. Thomas-Wohlever, J., and Lee, I. (2002) Kinetic characterization of the peptidase activity of *Escherichia coli* Lon reveals the mechanistic similarities in ATP-dependent hydrolysis of peptide and protein substrates, *Biochemistry 41*, 9418−9425.
23. Patterson, J., Vineyard, D., Thomas-Wohlever, J., Behshad, R., Burke, M., and Lee, I. (2004) Correlation of an adenine-specific conformational change with the ATP-dependent peptidase activity of *Escherichia coli* Lon, *Biochemistry 43*, 7432−7442.
24. Lee, I., and Berdis, A. J. (2001) Adenosine triphosphate-dependent degradation of a fluorescent λ N substrate mimic by Lon protease, *Anal. Biochem. 291*, 74−83.
25. Vineyard, D., Patterson-Ward, J., Berdis, A. J., and Lee, I. (2005) Monitoring the timing of ATP hydrolysis with activation of peptide cleavage in *Escherichia coli* Lon by transient kinetics, *Biochemistry 44*, 1671−1682.
26. Menon, A. S., and Goldberg, A. L. (1987) Binding of nucleotides to the ATP-dependent protease La from *Escherichia coli*, *J. Biol. Chem. 262*, 14921−14928.
27. Jia, Y., Kumar, A., and Patel, S. S. (1996) Equilibrium and stopped-flow kinetic studies of interaction between T7 RNA polymerase and its promoters measured by protein and 2-amino-purine fluorescence changes, *J. Biol. Chem. 271*, 30451−30458.
28. Gilbert, S. P., and Mackey, A. T. (2000) Kinetics: A tool to study molecular motors, *Methods 22*, 337−354.
29. Wong, I., and Lohman, T. M. (1993) A double-filter method for nitrocellulose-filter binding: Application to protein−nucleic acid interactions, *Proc. Natl. Acad. Sci. U.S.A. 90*, 5428−5432.
30. Bhattacharyya, J., and Das, K. P. (1999) Molecular chaperone-like properties of an unfolded protein, α(s)-casein, *J. Biol. Chem. 274*, 15505−15509.
31. Creamer, L. K., Richardson, T., and Parry, D. A. (1981) Secondary structure of bovine α s1- and β-casein in solution, *Arch. Biochem. Biophys. 211*, 689−696.
32. Kim, D. E., and Patel, S. S. (1999) The mechanism of ATP hydrolysis at the noncatalytic sites of the transcription termination factor Rho, *J. Biol. Chem. 274*, 32667−32671.
33. Stitt, B. L., and Xu, Y. (1998) Sequential hydrolysis of ATP molecules bound in interacting catalytic sites of *Escherichia coli* transcription termination protein Rho, *J. Biol. Chem. 273*, 26477−26486.
34. Yang, R., Cui, L., Hou, Y. X., Riordan, J. R., and Chang, X. B. (2003) ATP binding to the first nucleotide binding domain of multidrug resistance-associated protein plays a regulatory role at low nucleotide concentration, whereas ATP hydrolysis at the second plays a dominant role in ATP-dependent leukotriene C4 transport, *J. Biol. Chem. 278*, 30764−30771.
35. Sauna, Z. E., and Ambudkar, S. V. (2000) Evidence for a requirement for ATP hydrolysis at two distinct steps during a single turnover of the catalytic cycle of human *P*-glycoprotein, *Proc. Natl. Acad. Sci. U.S.A. 97*, 2515−2520.
36. Weber, J., and Senior, A. E. (2001) Bi-site catalysis in F1-ATPase: Does it exist? *J. Biol. Chem. 276*, 35422−35428.
37. Linnertz, H., Urbanova, P., and Amler, E. (1997) Quenching of 7-chloro-4-nitrobenzo-2-oxa-1,3-diazole-modified Na^+/K^+-ATPase reveals a higher accessibility of the low-affinity ATP-binding site, *FEBS Lett. 419*, 227−230.
38. Harkins, T. T., Lewis, T. J., and Lindsley, J. E. (1998) Pre-steady-state analysis of ATP hydrolysis by *Saccharomyces cerevisiae* DNA topoisomerase II. 2. Kinetic mechanism for the sequential hydrolysis of two ATP, *Biochemistry 37*, 7299−7312.
39. Harkins, T. T., and Lindsley, J. E. (1998) Pre-steady-state analysis of ATP hydrolysis by *Saccharomyces cerevisiae* DNA topoisomerase II. 1. A DNA-dependent burst in ATP hydrolysis, *Biochemistry 37*, 7292−7298.
40. Wong, I., and Lohman, T. M. (1997) A two-site mechanism for ATP hydrolysis by the asymmetric Rep dimer P2S as revealed by site-specific inhibition with ADP-A1F4, *Biochemistry 36*, 3115−3125.

BI052377T